Eur. Phys. J. D **30**, 71–79 (2004)
DOI: 10.1140/epjd/e2004-00072-8

THE EUROPEAN PHYSICAL JOURNAL D

# Global minima for free $Pt_N$ clusters (N = 22−56): a comparison between the searches with a molecular dynamics approach and a basin-hopping algorithm

A. Sebetci[1,a] and Z.B. Güvenç[2,b]

[1] Department of Computer Engineering, Çankaya University, 06530 Balgat Ankara, Turkey
[2] Department of Electronic and Communication Engineering, Çankaya University, 06530 Balgat Ankara, Turkey

Received 5 February 2004 / Received in final form 30 March 2004
Published online 18 May 2004 – 

**Abstract.** Using molecular dynamics and thermal quenching simulation techniques, and the basin-hopping Monte Carlo algorithm we have studied the global minima and energetics of free $Pt_N$ clusters in the size range of $N = 22-56$. The clusters have been described by the Voter and Chen version of an embedded-atom model, which is derived by fitting to experimental data of both the diatomic molecule and bulk platinum simultaneously. A comparison between the two search techniques has been performed and it is found that the basin-hopping algorithm is more efficient than a molecular dynamics minimization approach in the investigation of the global minima. The results show that the global minima of the Pt clusters have structures based on either octahedral, decahedral or icosahedral packing. Some of the icosahedral global minima do not have a central atom. The 54-atom icosahedron without a central atom is found to be more stable than the 55-atom complete icosahedron. The resulting structures have been compared with the previous theoretical calculations.

**PACS.** 36.40.-c Atomic and molecular clusters – 61.46.+w Nanoscale materials: clusters, nanoparticles, nanotubes, and nanocrystals

## 1 Introduction

In a recent paper [1] we have reported molecular dynamics (MD) studies of the energetics, structures, and probabilities of getting different basins of attractions of small, unsupported Pt clusters in the size range of $N = 2-21$, carried out using Voter and Chen version of an embedded-atom model (EAM) potential. Therefore, we do not repeat here a similar introductory part, the interaction potential and all the relevant references given in reference [1]. In the present work we report the global minima and energetics of free $Pt_N$ clusters of the sizes, $N = 22-56$, obtained by incorporating the same potential and using the same MD and thermal quenching (TQ) techniques described in reference [1], and using the basin-hopping algorithm of Wales and Doye [2], which is based upon Li and Scheraga's Monte Carlo (MC) minimization [3] approach. We have compared the two search techniques. The computational procedure will be given briefly in Section 2. Results and discussions are presented in Section 3, and conclusions are presented in Section 4.

[a] e-mail: asebetci@cankaya.edu.tr
[b] e-mail: guvenc@cankaya.edu.tr

## 2 Computational procedure

In the previous study [1], in order to obtain the lowest energy and the other locally stable structures of free Pt clusters, we generated 10,000 independent initial configurations for each size of the clusters by recording phase-space coordinates along high-energy trajectories. This method of consideration of a large number of initial configurations is reasonable only for small sizes since the number of isomers of a cluster increases exponentially as the number of atoms in the cluster increases.

In this work, search of the global minima of the larger sizes ($N \geq 22$) with MD and TQ techniques has been done in two phases. In the first phase, initially 500 independent configurations prepared along high-energy trajectories (about 2600 K) have been quenched to obtain a first candidate for the global minimum structure for each size of the clusters (in this size range we limit the number of independent initial conditions to 500 since further steps of the search are highly computationally demanding). After that, internal kinetic energies of these first candidates of the global minima have been increased in a stepwise manner and their short-time average internal kinetic energies (STKE) are monitored as a function of time at different total energies. Any transition from one

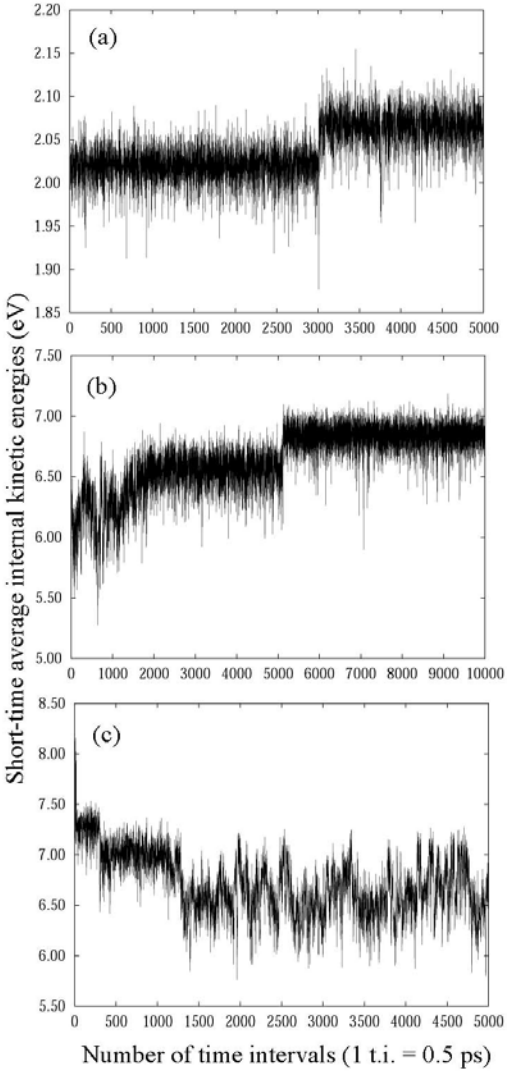


**Fig. 1.** The short-time average internal kinetic energies versus time graphs of $Pt_{55}$ clusters (a) for the first candidate at 297 K, (b) for the second candidate at 969 K, (c) for the global minimum structure at 979 K.

of the basins of attraction to another one affects the internal kinetic energy. Therefore, any phase change can be detected as an abrupt change in STKE as shown in Figure 1. When the total energy is high enough to pass over the barrier between the basins, clusters change their basins of attraction. If there is a lower energetic locally stable structure near the current basin of attraction of the cluster, that lower energetic basin of attraction biases the motion of the atoms in the phase space towards itself. Thus, whenever a jump to a higher STKE is observed, this new energetically lower isomer is considered as the second candidate for the global minimum structure and it is quenched and then heated gradually again. By repeating these quenching, heating, and monitoring processes we have searched a descending sequence of local minima for each size. The STKE of $Pt_{55}$ clusters for the first, second candidates and that of the global minimum structure are given in Figures 1a, 1b and 1c, respectively. In Figures 1a and 1b there are jumps indicating the changes of the current basins of attraction to the neighboring energetically lower basins of attraction. However, the STKE of the global minimum structure of $Pt_{55}$ cluster given in Figure 1c never climbs over its initial kinetic energy during the same amount of observation time. Instead, it starts to visit the neighboring higher potential energy wells. The method of the successive quenching and reheating of the MD phases described here has been used before for the Pd clusters by Karabacak et al. [4], and for the Cu clusters by Özçelik and Güvenç [5].

A descending sequence of local minima terminates at a particular potential well from which no further descent is possible. This bottom structure is the lowest-energy structure of that "funnel". However, there may be more than one "funnel" in a potential energy surface (PES) [6]. Namely, the descending sequences of local minima started from different initial configurations can terminate at different bottom structures. Different "funnels" are related to different structural morphologies. If the correct "funnel" is missed in the preparation of the 500 initial configurations, the real global minima may not be catched by the described procedure. Since as it is phrased by Wales and Doye [2] that "The most obvious short-cut would be to start not from initial random configurations but from seeds with either decahedral, icosahedral or fcc morphologies", in order to investigate the other possible "funnels" which may possess the global minimum structure, we have performed the second phase of our calculations in which two things have been done:

1. we have compared our results with the Monte Carlo minimization (or basin-hopping algorithm) study carried out using Sutten-Chen (SC) potentials by Doye and Wales [7]. We found that their 37-, 38-, 42-, 44-, and 50-atom structures have lower potential energies than our initial results. Therefore, we repeat the first phase of our calculations for these sizes by starting from the structures reported in reference [7]. Another study of Pt, Pd and Pt−Pd bimetallic clusters, with up to 56 atoms, performed by Johnston and co-workers [8] can also be considered for the comparison. Johnston and co-workers have reported the global minima for the mentioned clusters using the many-body Gupta potential [9] in their genetic algorithm calculations. Since the most of their structures are very similar to those found by Doye and Wales, we have been contented with the first comparison;
2. whenever the morphology of the global minimum structure of a size $N$ is different from the morphology of the neighboring sizes, $N-1$ and/or $N+1$, we have examined structure of the size $N$ in the form of neighboring size morphology. By this second consideration we have found lower energetic structures for 51-, 53-, and 54-atom clusters. Finally, we have applied the same heating, monitoring and quenching procedure to these new 8 structures ($N = 37$, 38, 42, 44, 50, 51, 53, and 54) once more. In only STKE of the 44-atom structure we have observed a small jump at about 650 K.

After quenching this new lower energetic structure, we have obtained the final putative global minimum structure of this size.

Most of the failures in the investigation of the global minima in the first phase of our calculations are due to the topographies of the potential energy surfaces (PES) which are likely to have multiple "funnels" in these 8 sizes [10] and due to computationally limited search time. To emphasize how difficult to find the lowest energy structure in certain sizes, we have performed the following calculations: the quasi-Newton L-BFGS routine [11] is added to our MD program. And then, starting from a random initial configuration, we let the 38-atom Pt cluster takes 10 million time steps in the phase space at about 2700 K. After each MD step, the L-BFGS routine is called to relax the cluster into the nearest local minima by minimizing the cluster potential energy as a function of the coordinates of the atoms. In some cases the routine could not perform the minimization process due to the fact that the numerical form of the potential as an interpolation array is not defined for very small and very large scalar distances to neighboring atoms. Within the 8,596,259 successful minimizations, 127,510 different local minima were found. During the whole trip the basin of attraction of the lowest energy structure (truncated octahedron) was visited only 1012 times. Therefore, if we had chosen randomly 10,000 (nearly equal to 10 million/1012) sets of configurations among 10 million sets produced in the MD trajectory and if we had used them as our initial configurations in the first phase of our calculations, only one of them would have ended up with the global minimum structure, on average.

In order to test the results found by the MD global minimization approach described above, we have also applied a recognized global optimization method, basin-hopping MC algorithm, to this problem and the GMIN [12] program is used to locate the lowest energy structures of the Voter-Chen Pt clusters. The details of the algorithm can be found in reference [2]. We have started to the MC runs with the configurations which are the global minimum structures of the Morse clusters. For a given size, as the interaction range of the Morse potential changes, the global minimum changes. The different global minima for different interaction ranges of the Morse potential have been reported by Doye and Wales up to 80-atom clusters before [13,14]. We have reoptimized all the Morse global minima by performing several MC runs of 100,000 steps of each. We use A, A', B, B', ... notations to keep track the Morse global minima. We report those Morse global minima that result in the global minimum structure of the corresponding Voter-Chen Pt clusters, in Table 1. All of the lowest energy structures found in the MD search are also found by the MC search as well. However, the basin-hopping algorithm has found lower energetic structures of three sizes, $N = 42$, 51, and 52, which could not be found by the MD search in spite of all considerations mentioned above. Therefore, it is obvious that the basin-hopping algorithm is more suitable for searching the global minima of the potential energy landscapes of the atomic clusters than an MD and TQ approaches.

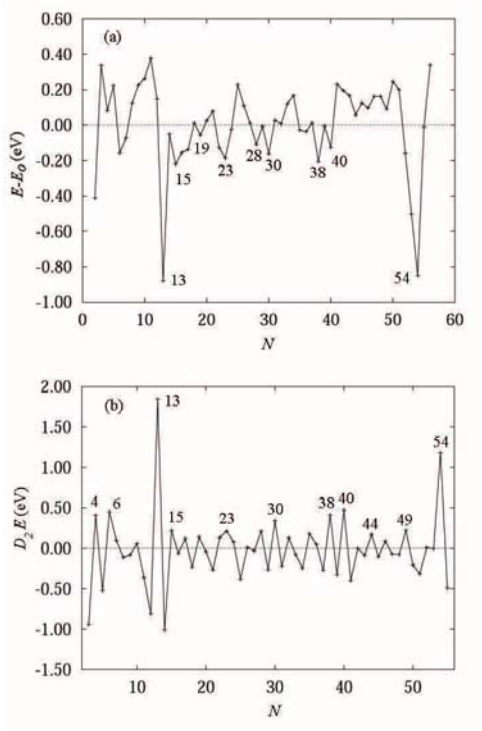


**Fig. 2.** (a) Energies where $E_0 = 13.2571 - 11.4405N^{1/3} + 6.83048N^{2/3} - 6.21779N$. (b) The second finite difference in binding energy.

We discuss the morphologies of the global minima in the next section. Although no one can be sure that the true global minima were obtained, the structures presented here can be considered, at least, as good starting points for further investigations and illuminate the growth path of the clusters. All our published results are available on request.

## 3 Results and discussion

We have reported the total energies ($E$), energies per particle ($E/N$), the Morse global minima ($MGM$) which is used to seed the MC runs and result in the lowest energy structure, the point groups ($PG$), the structural assignments ($SA$), the average bond lengths ($R_b$) and the differences between the maximum and minimum bond lengths ($D_R$) of all the global minima in Table 1. The point groups of the structures are determined with OPTIM program [12]. Symmetry elements are diagnosed when rotation and reflection operators produce the same geometry (correct to 0.01) in each Cartesian coordinates. We have also indicated the global minima in Table 1 if they are common with SC Pt clusters reported in reference [7]. The energies and the second finite differences in energies

$$D_2E(N) = E_l(N+1) + E_l(N-1) - 2E_l(N) \quad (1)$$

are plotted in Figures 2a and 2b, respectively. For the sake of completeness we have included the energies of the

**Table 1.** Results for global minima of $Pt_{22} - Pt_{56}$ clusters.

| $N^a$ | $E^b$ | $E/N^c$ | $MGM^d$ | $PG^e$ | $SA^f$ | ${R_b}^g$ | ${D_R}^h$ |
|---|---|---|---|---|---|---|---|
| 22 | −102.088 | −4.640 | A, B | $C_1$ | face-sharing icosahedral | 2.642 | 0.520 |
| 23 | −107.231 | −4.662 | A, B, C, D | $C_2$ | face-sharing icosahedral [i] | 2.650 | 0.572 |
| 24 | −112.161 | −4.673 | A, A', B, C | $C_s$ | face-sharing icosahedral [i] | 2.630 | 0.325 |
| 25 | −117.011 | −4.680 | A, A', B, C | $C_3$ | face-sharing icosahedral | 2.664 | 0.606 |
| 26 | −122.241 | −4.702 | A, B, C | $C_1$ | face-sharing icosahedral | 2.659 | 0.633 |
| 27 | −127.459 | −4.721 | A, B, C | $C_s$ | face-sharing icosahedral | 2.662 | 0.591 |
| 28 | −132.707 | −4.740 | A, B, C, D, E | $C_s$ | face-sharing icosahedral | 2.645 | 0.613 |
| 29 | −137.741 | −4.750 | A, B, C, D, E, F | $C_2$ | face-sharing icosahedral [i] | 2.645 | 0.466 |
| 30 | −143.039 | −4.770 | A, B, C, D, D', E | $C_{3v}$ | face-sharing icosahedral [i] | 2.650 | 0.370 |
| 31 | −147.999 | −4.774 | A, B, C, D, E, F | $C_3$ | face-sharing icosahedral | 2.679 | 0.540 |
| 32 | −153.179 | −4.787 | A, B, C, D, E | $D_{2d}$ | face-sharing icosahedral | 2.660 | 0.516 |
| 33 | −158.230 | −4.795 | A, B, C, D, E, F | $C_2$ | face-sharing icosahedral | 2.659 | 0.514 |
| 34 | −163.357 | −4.801 | A, B, C, D, E, F | $C_s$ | face-sharing icosahedral | 2.654 | 0.578 |
| 35 | −168.730 | −4.821 | A, B, C, D, E, F | $D_3$ | face-sharing icosahedral | 2.668 | 0.529 |
| 36 | −173.924 | −4.831 | A, B, C, D, E, F, G | $C_{2v}$ | face-sharing icosahedral [i] | 2.647 | 0.357 |
| 37 | −179.068 | −4.840 | A, B, C, D, E | $C_{2v}$ | decahedral [i] | 2.677 | 0.343 |
| 38 | −184.483 | −4.855 | A, B, C, D, E | $O_h$ | truncated octahedron [i] | 2.679 | 0.180 |
| 39 | −189.486 | −4.859 | A, B, C | $C_s$ | centred icosahedral | 2.660 | 0.481 |
| 40 | −194.816 | −4.870 | A, B, C | $D_2$ | face-sharing icosahedral | 2.670 | 0.439 |
| 41 | −199.675 | −4.870 | A, B, C, D, E, F | $C_1$ | centred icosahedral | 2.661 | 0.552 |
| 42 | −204.930 | −4.879 | A, B, C, D, E | $C_4$ | face-sharing icosahedral | 2.656 | 0.340 |
| 43 | −210.185 | −4.888 | A, B, C, D, E | $C_2$ | centred icosahedral | 2.661 | 0.537 |
| 44 | −215.526 | −4.898 | A, B, C, D, E | $C_1$ | centred icosahedral | 2.671 | 0.597 |
| 45 | −220.694 | −4.904 | A, B', C, D, E, F | $C_s$ | centred icosahedral [i] | 2.657 | 0.490 |
| 46 | −225.965 | −4.912 | A, B, C, D, E, E' | $C_s$ | centred icosahedral | 2.672 | 0.529 |
| 47 | −231.146 | −4.918 | A, B, C, D | $C_1$ | centred icosahedral | 2.674 | 0.615 |
| 48 | −236.397 | −4.925 | A, B, B', C, D | $C_1$ | centred icosahedral [i] | 2.672 | 0.607 |
| 49 | −241.724 | −4.933 | A, B, C, D | $C_1$ | centred icosahedral | 2.670 | 0.551 |
| 50 | −246.830 | −4.937 | D | $D_{3h}$ | truncated octahedral [i] | 2.689 | 0.196 |
| 51 | −252.140 | −4.944 | E | $C_{3v}$ | uncentred icosahedral | 2.663 | 0.219 |
| 52 | −257.768 | −4.957 | B | $C_{2h}$ | uncentred icosahedral | 2.665 | 0.223 |
| 53 | −263.386 | −4.970 | A, B, C | $C_{5v}$ | uncentred icosahedral | 2.667 | 0.238 |
| 54 | −269.011 | −4.982 | A, B, C, D | $I_h$ | uncentred icosahedron | 2.670 | 0.202 |
| 55 | −273.454 | −4.972 | A, B, C, D | $I_h$ | centred icosahedron | 2.686 | 0.183 |
| 56 | −278.389 | −4.971 | A, B, C, D, E | $C_s$ | uncentred icosahedral | 2.671 | 0.501 |

[a] Size. [b] Energy (eV). [c] Energy per particle (eV). [d] Morse global minima [29] which result in the global minimum of Pt cluster when they are reoptimized. [e] Point group. [f] Structural assignment. [g] Average bond length (Å). [h] Difference between max. and min. bond lengths (Å). [i] Common with Sutton-Chen structures given in reference [7].

sizes $N = 2-21$ into these two graphs. Following Northby et al. [15] and Lee and Stein [16], the function,

$$E_0 = aN + bN^{2/3} + cN^{1/3} + d, \qquad (2)$$

is fitted to the energies given in Table 1, and it is subtracted from the energies of the clusters in order to emphasize the size dependence. In this polynomial function, $a$ describes the volume, $b$ surface, $c$ edge, and $d$ the vertex contributions to the energy. $D_2E$ is generally correlated with the magic numbers observed in mass spectra. Clusters are particularly abundant at magic number sizes in mass spectra since they are the most stable ones [17].

The core, the surface and the triangulated polyhedral surface structures of the $Pt_{22} - Pt_{39}$ global minima are illustrated in Figure 3 and those of the $Pt_{40} - Pt_{56}$ global minima are in Figure 4. We call an atom in a cluster as a core-atom if its coordination number ($CN$), which is the number of neighbors within a cutoff radius $1.2r_e$, is greater than or equal to 10. The $r_e$ (2.78 Å) is the nearest

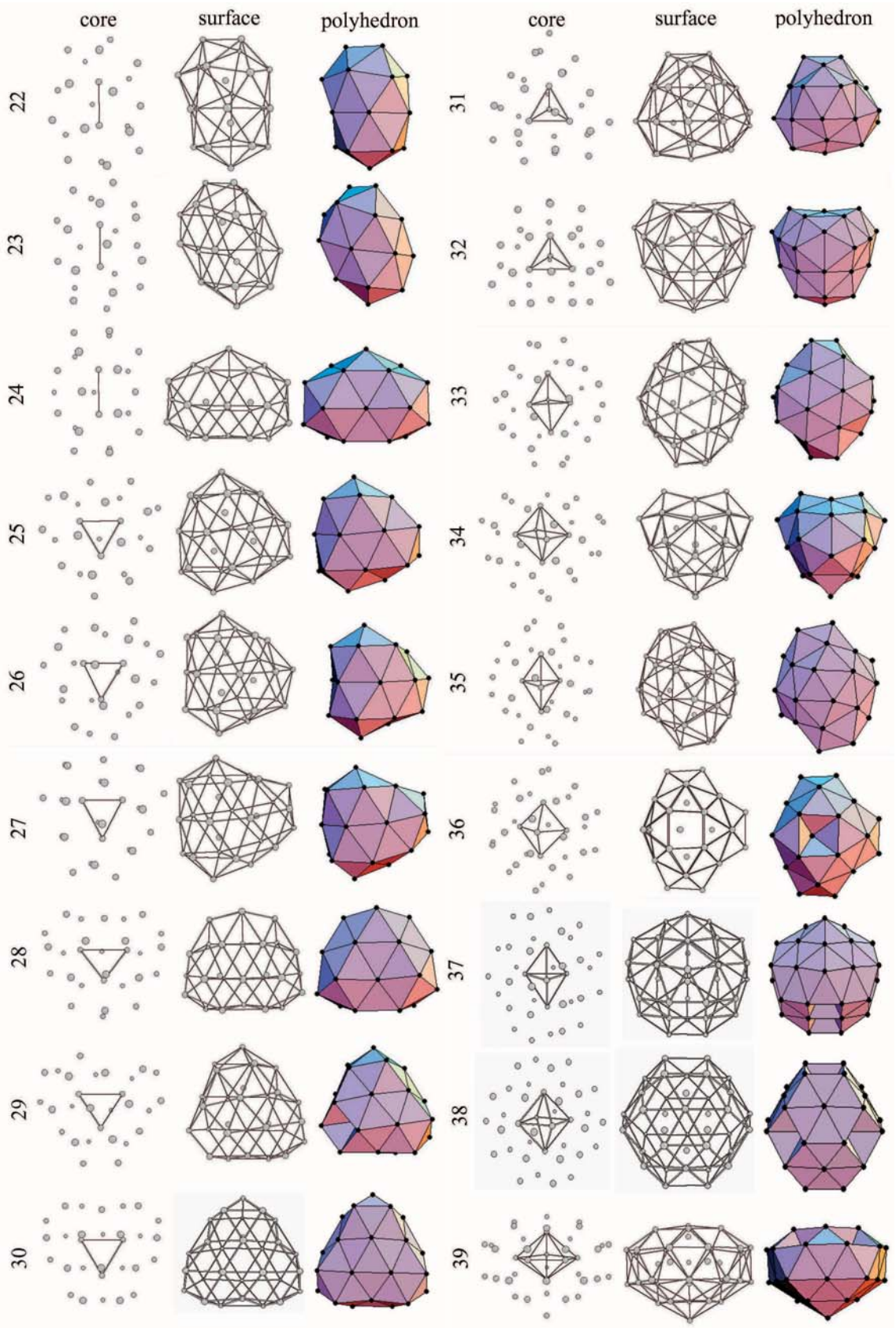


**Fig. 3.** Global minima for $Pt_{22} - Pt_{39}$ clusters.

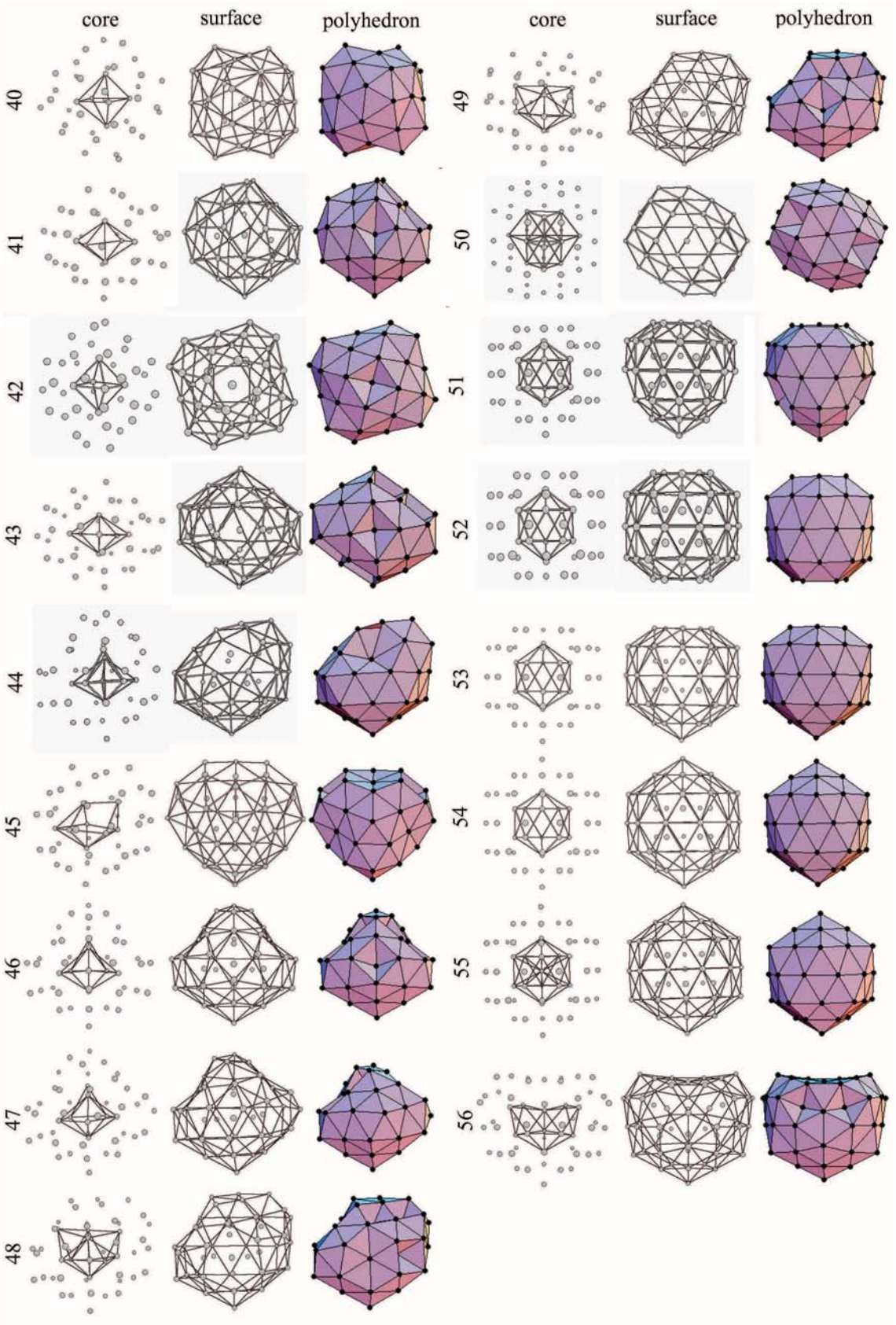


**Fig. 4.** Global minima for $Pt_{40} - Pt_{56}$ clusters.

**Table 2.** Coordination number analysis of $Pt_{22}-Pt_{56}$ clusters.

| Size | Coordination number | | | | | | | | | |
|---|---|---|---|---|---|---|---|---|---|---|
| $N$ | 5 | 6 | 7 | 8 | 9 | 10 | 11 | 12 | 13 | 14 |
| 22 | 0 | 13 | 5 | 2 | 0 | 0 | 0 | 1 | 1 | 0 |
| 23 | 0 | 12 | 6 | 3 | 0 | 0 | 0 | 0 | 2 | 0 |
| 24 | 1 | 14 | 5 | 2 | 0 | 0 | 0 | 0 | 2 | 0 |
| 25 | 0 | 12 | 3 | 6 | 1 | 0 | 0 | 3 | 0 | 0 |
| 26 | 0 | 13 | 4 | 5 | 1 | 0 | 0 | 2 | 1 | 0 |
| 27 | 0 | 13 | 4 | 7 | 0 | 0 | 1 | 0 | 1 | 1 |
| 28 | 1 | 12 | 8 | 4 | 0 | 0 | 1 | 0 | 2 | 0 |
| 29 | 2 | 12 | 6 | 6 | 0 | 0 | 0 | 1 | 2 | 0 |
| 30 | 0 | 12 | 9 | 6 | 0 | 0 | 0 | 0 | 3 | 0 |
| 31 | 0 | 12 | 6 | 6 | 3 | 0 | 0 | 1 | 3 | 0 |
| 32 | 0 | 12 | 12 | 0 | 4 | 0 | 0 | 4 | 0 | 0 |
| 33 | 2 | 10 | 8 | 8 | 0 | 1 | 0 | 4 | 0 | 0 |
| 34 | 1 | 13 | 10 | 4 | 0 | 2 | 1 | 3 | 0 | 0 |
| 35 | 0 | 12 | 6 | 12 | 0 | 0 | 0 | 5 | 0 | 0 |
| 36 | 0 | 16 | 6 | 9 | 0 | 0 | 4 | 1 | 0 | 0 |
| 37 | 2 | 18 | 2 | 10 | 0 | 0 | 0 | 5 | 0 | 0 |
| 38 | 0 | 24 | 0 | 0 | 8 | 0 | 0 | 6 | 0 | 0 |
| 39 | 0 | 15 | 7 | 10 | 0 | 0 | 3 | 4 | 0 | 0 |
| 40 | 0 | 12 | 8 | 14 | 0 | 0 | 0 | 6 | 0 | 0 |
| 41 | 1 | 17 | 5 | 10 | 2 | 0 | 0 | 4 | 2 | 0 |
| 42 | 0 | 16 | 8 | 12 | 0 | 0 | 0 | 6 | 0 | 0 |
| 43 | 0 | 18 | 6 | 12 | 0 | 0 | 2 | 3 | 2 | 0 |
| 44 | 0 | 15 | 8 | 12 | 1 | 1 | 0 | 5 | 1 | 1 |
| 45 | 2 | 14 | 6 | 15 | 0 | 2 | 4 | 2 | 0 | 0 |
| 46 | 0 | 16 | 6 | 14 | 2 | 0 | 1 | 4 | 3 | 0 |
| 47 | 0 | 14 | 7 | 17 | 1 | 0 | 1 | 6 | 1 | 0 |
| 48 | 0 | 18 | 5 | 15 | 0 | 2 | 1 | 3 | 4 | 0 |
| 49 | 0 | 17 | 4 | 18 | 0 | 1 | 3 | 5 | 1 | 0 |
| 50 | 0 | 24 | 6 | 0 | 8 | 3 | 0 | 9 | 0 | 0 |
| 51 | 0 | 9 | 15 | 15 | 0 | 3 | 9 | 0 | 0 | 0 |
| 52 | 0 | 10 | 10 | 20 | 0 | 2 | 10 | 0 | 0 | 0 |
| 53 | 0 | 11 | 5 | 25 | 0 | 1 | 11 | 0 | 0 | 0 |
| 54 | 0 | 12 | 0 | 30 | 0 | 0 | 12 | 0 | 0 | 0 |
| 55 | 0 | 12 | 0 | 30 | 0 | 0 | 0 | 13 | 0 | 0 |
| 56 | 0 | 15 | 7 | 21 | 2 | 0 | 7 | 4 | 0 | 0 |

neighbor distance in the perfect crystal. The atoms with $5 \leq CN \leq 9$ are called as surface atoms and the atoms with $CN = 3-4$ are called as capping atoms. Definitions of the core and surface atoms given here are slightly different from those of Lee and co-workers [18]. They named the atoms with $CN = 10$ as surface atoms. The $CN$ analysis of all the global minima is given in Table 2. In Figures 3 and 4, the bonds between the core and surface atoms are not presented to make the figures clearer. Furthermore, all the surface and the triangulated polyhedral structures are presented from the same points of view, whereas the figures of the structures which show explicitly the cores are rotated as a whole with respect to the remaining two figures by arbitrary angles to get the best view of the core part.

From Figure 2a it can be seen that the most stable structures occur at sizes 13 and 54. The 13-atom structure is a complete Mackay icosahedron [19] as we reported in our previous work [1], whereas the 54-atom structure is a Mackay icosahedron without a central atom. The icosahedral morphology without the central atom in the global minima of the Pt clusters starts at the size of 51 and continues up to the size of 56 except the 55-atom structure which is a centred icosahedron. Since the icosahedral morphologies with and without a central atom have their own "funnels", we have found only one uncentred icosahedral 52-atom cluster and the 56-atom global minimum at the end of the first phase of our MD calculations. Initially, the 51-, 53-, and 54-atom putative global minima had been found as some structures belonging to the centred icosahedral morphology. For instance, the 54-atom structure was a complete 55-atom icosahedron with a missing one of the surface atoms among the ones having the least $CN$. After examining the uncentred icosahedral "funnel" in the MD search, we have found some uncentred icosahedral local minima of the sizes of $N = 51$, 53 and 54 too, which are lower in energy than their centred icosahedral structures. However, the structures of the sizes of $N = 51$ and 52 found in the MD search have been improved in the basin-hopping MC search. The global minima of the 51- and 52-atom clusters are uncentred icosahedra missing 3 and 2 surface atoms respectively (the missing atoms are on the opposite sides of the clusters, see Fig. 4). In the MD search these missing atoms are found to be closer to each other.

The energy difference between the 54-atom uncentred icosahedron and the 54-atom centred icosahedron with missing one surface atom is more than 1 eV. Although a central atom in an icosahedron has 12 $CN$, which is greater than the $CN$ of any surface or capping atoms, the uncentred 54-atom icosahedron has lower energy than the 54-atom icosahedron with a central atom. This is because of the fact that the central atom pushes the other atoms outwards and the spherical shells expand. The radius of the inner shell of the 55-atom complete icosahedron is 2.6095 Å. The distances between the central atom and the surface atoms having 6 and 8 $CN$ are 4.4653 Å and 5.1126 Å, respectively. However, the corresponding distances in the 54-atom uncentred icosahedron are 2.5207 Å, 4.4317 Å, and 5.0578 Å, which are all smaller. An other comparison can be made between the average bond lengths of the 54-atom structures having no central atom and missing one surface atom. The average bond length of the 54-atom global minimum structure (the uncentred icosahedron) is 0.015 Å less than that of the 54-atom centred icosahedron missing a surface atom. A perfect 55-atom Pt icosahedron has four topologically different types of atoms: a central atom, the atoms on the inner shell, the atoms on the outer shell with $CN = 6$ and those with $CN = 8$. The potential energies of each of these four types of atoms are $-5.215$ eV, $-5.420$ eV, $-4.392$ eV, and $-5.017$ eV, respectively. Therefore, extracting an atom from the center requires more energy than extracting an atom from the surface. In other words,

the total potential energy of an icosahedron with a point defect at the center is higher than that of the icosahedron with a point defect on the surface, if all the interatomic distances are retained in their original values after the defects are created. However, when the defected structures relax, the uncentred icosahedron becomes less energetic than the centred icosahedron missing a surface atom.

Global minima of all the clusters from 51-atom to 54-atom have the same structure in their cores, i.e., a 12-atom uncentred icosahedron. The 12-atom uncentred icosahedron is stable at low temperatures but its energy is not lower than the global minimum structure of the 12-atom centred icosahedral cluster that we reported before [1]. The 12-atom uncentred icosahedron of gold cluster is reported as the global minimum structure by Wilson and Johnston [20] in their MD simulated annealing study carried out using an empirical Murrell-Mottram many-body potential function. Our uncentred icosahedral global minima of the 51-, 52-, 53-, and 54-atom clusters are stable up to about 650 K, 810 K, 790 K, and 1000 K, respectively. The energy of the uncentred icosahedral isomer of the 55-atom cluster, which has 6 atoms instead of 5 in one of the smaller rings on either pole of the uncentred icosahedron, is about 0.1 eV higher than that of the global minimum structure (55-atom centred icosahedron). The core of the global minimum structure of the 56-atom cluster is an uncentred 12-atom icosahedron with a missing atom from the surface of the core.

From Figure 2a it can be seen that the 54-atom uncentred icosahedron is more stable than the 55-atom centred icosahedron because its relative energy with respect to the reference energy $E_0$ is much lower than that of the 55-atom structure. Similarly, Figure 2b shows that intensity of the 54-atom clusters in a mass spectrum should be much higher than that of the 55-atom clusters. However, one should note that the experimental conditions range from rapid cooling (mostly kinetic control) to long periods of heat treatment (mostly thermodynamic control) [21]. Since the global minima of the most of the smaller clusters have centred icosahedral morphology, as the Pt atoms aggregate in the laboratory conditions to form higher sizes, the structures having a central atom would be observed initially. It could take a relatively long time for a central atom to escape to the surface of the structure even if it has enough energy. Therefore, under kinetically controlled conditions, one would expect to find that the 55-atom centered icosahedron is more favorable in the mass spectra. On the other hand, if the experiments are mostly thermodynamic control in nature the global minimum structures should be observed, therefore, we would expect to find similar results to the ones that we report here in such conditions. Unfortunately we cannot find any experimental study on the structures or mass spectra of the bare Pt clusters in the size regime considered here except the one performed by Andersson and Rosen [22]. They have reported the mass spectra of both bare Pt clusters and of the Pt clusters with adsorbed hydrogen (deuterium) and oxygen molecules in the size range between 7- and 30-atom. However, they haven't observed any size effect in their mass spectra of the bare Pt clusters (in the size range of 10−16) which does not correlate well not only with our $D_2E$ given in Figure 2b but also corresponding the second difference in binding energy calculations of both Doye and Wales [7] and of Johnston and co-workers [8]. There are some experimental studies on the structures of Ni clusters by Riley and co-workers [23–26]. Using nitrogen probe molecules, they have reported the global minimum structures of the 38- and 55-atom Ni clusters as truncated octahedron [25] and centred icosahedron [26], respectively, which are similar to our results for the corresponding Pt clusters. We could not find any experimental evidence for the 54-atom uncentred icosahedral structure of the metal clusters among the existing experimental studies, therefore, we believe that it should be taken into consideration and studied under proper conditions. We are also aware of the fact that at present it is often not possible to determine the structures of clusters unambiguously in the gas phase or in a molecular beam [27].

There are some shallow minima in the energy plot [Fig. 2a] at $N = 15$, 19, 23, 28, 30, 38, and 40. We have reported before [1] the 15- and 19-atom global minima as a hexagonal bipyramid and a double icosahedron, respectively. The 23- and 30-atom global minima are common with SC gold and platinum clusters. The 23-atom structure resembles the 23-atom SC silver and rhodium global minima [7]. All of the 22-, 23- and 24-atom global minima have two atoms in their cores. These structures can be classified as two distorted phase-sharing icosahedra. All of the clusters between the sizes of $N = 25$ and $N = 30$ have three atoms in their cores. These structures may be called as three distorted phase-sharing icosahedra. The 30-atom structure is made up of three interpenetrating $D_{3h}$ units. The global minima of the clusters from the 31- to 36-atom also consist of several distorted icosahedra. The 37- and 38-atom structures are borrowed from reference [7]. The first is a distorted decahedron and the second one is a truncated octahedron. The 37-atom structure is the only structure belonging to the decahedral morphology in our calculations. The 40-atom structure may be related to the 38-atom icosahedral structure given in reference [28]. We have found the same 38-atom icosahedral structure at the end of the first phase of our calculations. However, the 38-atom truncated octahedron has 0.1832 eV lower in energy than the 38-atom icosahedral structure. Since this energy difference is small for the $N = 38$ (it is almost a degenerate state), the dip and the peak in Figure 2 for this size are not well pronounced. The 39-, and from the 41- to 49-atom clusters contain a pentagonal bipyramids in their cores except the 42-atom cluster. They are all related to each others and have centred icosahedral morphology. The 42-atom global minimum could not be found by MD and TQ searches but it has been located by the basin-hopping algorithm. It is a face-sharing icosahedron containing a 6-atom octahedron in its core. The 50-atom global minimum is the "twinned truncated octahedron" (the coordinates were taken from The Cambridge Cluster Database [29] mentioned in Ref. [7]). In our initial calculations, we have found an icosahedral structure for this size.

The energy difference between the lowest energy structures of the icosahedral and the octahedral "funnels" of the 50-atom clusters is about 0.03116 eV, which is even smaller than the corresponding quantity of those of the above mentioned 38-atom clusters. Therefore, in Figure 2 there is no structure for the size of $N = 50$. Between the two perfect spherical symmetries at the sizes of $N = 13$ and $N = 54$, the energy difference between different morphologies of a given size is small. Thus, in Figures 2a and 2b these sizes are oscillating around the reference lines without any pronounced dips or peaks.

The Pt clusters described by Voter-Chen version of the EAM potential and SC potential have common global minima at 10 sizes ($N$ = 23, 24, 29, 30, 36, 37, 38, 45, 48 and 50). However, the EAM potential energies of these structures are significantly smaller than the SC potential energies for all of these sizes. For instance, the SC potential energy of the 23-atom global minimum structure is 118.814 eV, whereas the EAM potential energy of the same structure is 107.231 eV. The energy difference between the two models increases as the size increases, and it reaches up to 19.595 eV at $N = 50$. Both of Voter-Chen and SC potentials are spherically symmetric and both of them have many-body parts. The main difference between them is the fact that the Voter and Chen version of the EAM potential is derived by fitting simultaneously to the properties of the diatomic molecule and the bulk platinum, however the parameters of the SC potential are derived by fitting to those of only the bulk platinum. Therefore, we expect that the Voter and Chen's model is more suitable for the small clusters. This is the reason to explain different results of the global minima reported in this paper and in the reference [7].

## 4 Conclusions

In this paper, we have tried to find likely global minima for the free Pt clusters in the size range of $N = 22-56$ whose interactions are described by Voter and Chen version of the EAM potential. Using MD, TQ and basin-hopping MC techniques we have found out that all the global minima have one of the octahedral, decahedral, centred or uncentred icosahedral morphologies. Although the 38-atom global minimum structure is a truncated octahedron, 50-atom structure is a "twined truncated octahedron" and 37-atom structure is a distorted decahedron, the smaller sizes of all the other global minima have centred icosahedral and the larger ones have uncentred icosahedral morphologies. The 54-atom uncentred icosahedron is found to be more stable than 55-atom centred icosahedron. The basin-hopping minimization approach is more efficient for the investigation of the global minima of atomic clusters than an MD and TQ techniques.

We would like to thank to J.P.K. Doye for providing the Fortran code to find the point groups of the global minima and the small Mathematica notebook to draw the triangulated polyhedral figures.

## References

1. A. Sebetci, Z.B. Güvenç, Surf. Sci. **525**, 66 (2003); and references therein
2. D.J. Wales, J.P.K. Doye, J. Phys. Chem. A **101**, 5111 (1997)
3. Z. Li, H.A. Scheraga, Proc. Natl. Acad. Sci. USA **84**, 6611 (1987)
4. M. Karabacak, S. Özçelik, Z.B. Güvenç, Surf. Sci. **532-535**, 306 (2003)
5. S. Özçelik, Z.B. Güvenç, Surf. Sci. **532-535**, 312 (2003)
6. R.H. Leary, J. Glob. Opt. **18**, 367 (2000)
7. J.P.K. Doye, D.J. Wales, New J. Chem., 733 (1998)
8. C. Massen, T.V. Mortimer-Jones, R.L. Johnston, J. Chem. Soc., Dalton Trans. **23**, 4375 (2002)
9. F. Cleri, V. Rosato, Phys. Rev. B **48**, 22 (1993)
10. J.P.K. Doye, M.A. Miller, D.J. Wales, J. Chem. Phys. **111**, 8417 (1999)
11. R.H. Byrd, P. Lu, J. Nocedal, C. Zhu, SIAM J. Sci. Comput. **16**, 1190 (1995)
12. `http://www-wales.ch.cam.ac.uk/software.html`
13. J.P.K. Doye, D.J. Wales, R.S. Berry, J. Chem. Phys. **103**, 4234 (1995)
14. J.P.K. Doye, D.J. Wales, J. Chem. Soc., Faraday Trans. **93**, 4233 (1997)
15. J.A. Northby, J. Xie, D.L. Freeman, J.D. Doll, Z. Phys. D **12**, 69 (1989)
16. J.W. Lee, G.D. Stein, J. Phys. Chem. **91**, 2450 (1987)
17. K. Clemenger, Phys. Rev. B **32**, 1359 (1985)
18. Y.J. Lee, E.K. Lee, S. Kim, Pyhs. Rev. Lett. **86**, 999 (2001)
19. A.L. Mackay, Acta Crystallogr. **15**, 916 (1962)
20. N.T. Wilson, R.L. Johnston, Eur. Phys. J. D **12**, 161 (2000)
21. J. Uppenbrink, D.J. Wales, J. Chem. Phys. **96**, 8520 (1992)
22. M. Andersson, A. Rosen, J. Chem. Phys. **117**, 7051 (2002)
23. E.K. Parks, L. Zhu, J. Ho, S.J. Riley, J. Chem. Phys. **100**, 7206 (1994)
24. E.K. Parks, G.C. Nieman, K.P. Kerns, S.J. Riley, J. Chem. Phys. **108**, 3731 (1998)
25. E.K. Parks, S.J. Riley, Z. Phys. D **33**, 59 (1995)
26. E.K. Parks, B.J. Winter, T.D. Klots, S.J. Riley, J. Chem. Phys. **94**, 1882 (1991)
27. R.L. Johnston, *Atomic and Molecular Clusters* (Taylor and Francis, London, 2002)
28. N.T. Wilson, R.L. Johnston, Phys. Chem. Chem. Phys. **4**, 4168 (2002)
29. `http://brian.ch.cam.ac.uk/CCD.html`